Journal of the European Ceramic Society **15** (1995) 9–16

0955-2219/95/$9.50

Effect of Powder Granulometry and Pre-treatment on Sintering Behavior of Submicron-grained α-Alumina

Eiichi Sato* & Claude Carry‡

Laboratoire de Céramique, Ecole Polytechique Fédérale de Lausanne, MX-Ecublens, CH-1015 Lausanne, Switzerland

(Received 14 December 1993; revised version received 3 June 1994; accepted 13 June 1994)

Abstract

Two kinds of commercial, submicron-grained, non-doped α-alumina powders were cold-isostatically pressed and then sintered at a constant heating rate. Before the sintering, pre-treatments were executed at 820 or 920°C for 50 h. The effects of the pre-treatments on the densification behavior and the microstructural development are discussed.

The powders contained some nano-sized alumina particles about 10 nm in diameter as well as sub-micron-sized primary particles about 0·1 μm in diameter, which agglomerated in packs of 0·2–0·4 μm diameter. The densification rate curves showed a low temperature shoulder during sintering attributed to these nano-sized particles. After pre-treatments, the nano-particles disappeared, resulting in disappearance of the shoulder in the subsequent densification rate curves. These treatments, however, caused little change in the apparent activation energy in the intermediate stage sintering. For the weakly agglomerated powders, the bodies sintered with pre-treatments had coarser final microstructures.

1 Introduction

In order to obtain ceramics with pore-free, fine-grain structures by stress-free sintering, there is always a competition between densification and grain growth.[1] For nano-phase ceramics the competition is much more significant.[2] The main obstacles in obtaining ceramics with theoretical density have been attributed to nonuniformities in green bodies, and the particle size distribution and degree of agglomeration of the starting powder are the main origins of the nonuniformities.[3]

The packing of a powder with a bimodal particle size distribution can give a higher green density than a mono-sized powder, due to the effective interspace filling between coarse particles by fine particles.[4] In spite of the higher green density, enhanced densification in compacts prepared from powders with bimodal[5,6] or wide size distributions[7] has not been observed. This is because the shrinkage rate is primarily governed by the large grains,[8] and localized stresses developed around them prevented an enhanced densification.

A narrow size distribution, on the other hand, is thought to be important[9] because a uniform pore distribution results in sintering to high final densities.[10] It has been reported that both classification of powders[11] and controlled colloidal techniques[12] to obtain narrow-sized powders allow powder compacts to sinter more rapidly and to higher densities at lower temperatures than compacts made from conventional powders. It must be pointed out that the controlled colloidal techniques give powders not only narrow-sized but also agglomerate-free, the other factor often cited as a cause of inhomogeneities in green bodies.

Recently, Chu *et al.*[13] reported that pre-treatments of a green compact at a low temperature without densification produced a compact with a more uniform microstructure than the initial one. This kind of treatment provides an ideal stage to discuss the effect of granulometry on sintering behavior. They, however, gave neither detailed observation nor clear explanation on how the densification proceeded and the microstructure developed during the subsequent sintering. As another method of heat schedule, 'Rate-controlled sintering' (where the heating rate is decreased to avoid rapid shrinkage in the intermediate stage), has had practical success,[14] it should be fruitful to compare these two methods.

It is the purpose of the present paper to reveal the effects of powder granulometry and pretreat-

* On leave from the Institute of Space and Astronautical Science, 3-1-1 Yoshinodai, Sagamihara 229, Japan.
‡ Present address: Institut de Science des Matériaux, Université de Paris-Sud, Bâtiment 413, Centre d'Orsay, 91405 Orsay Cedex, France.

ments on sintering behavior and on microstructural development using non-doped, submicron-grained alumina powders with different particle size distributions as model materials. Adopting a constant heating rate condition allows the shrinkage behavior in the initial stage of sintering to be observed[15] and the apparent activation energy in the intermediate stage to be estimated.[16]

2 Experimental Procedure

Two kinds of commercial, submicron-grained, non-doped α-alumina powders were used: they are denoted by BO (CR15-AS1, Baikowski, France) and TA (TM-DR, Taimei Chemicals, Japan). The main impurities are Si, K, Na and Fe, for the BO powders of 57, 45, 10 and 7 mass ppm and for the TA powders of 10, 2, 2 and 8 mass ppm, respectively. Figure 1 shows the particle size distribution of the powders given by the suppliers. Both powders consist of mainly submicron-sized particles with median volume diameters of 0·2 μm (TA) and 0·4 μm (BO).

Green compacts were prepared by cold-isostatic pressing (CIP) at a pressure of 250 MPa. They were machined into cylindrical samples with 15 mm height and 10 mm diameter. Some of them were annealed in a chamber furnace in air at 820 or 920°C for 50 h; this will be referred to as a pretreatment. The treatment at 820°C caused almost no densification, and that at 920°C caused a small increase in the relative density of 0·02 for compacts of both powders.

The samples were sintered in a vertical dilatometer (DHT2050K, Setaram, France) under constant heating rate conditions at various rates from 1·0 to 10°C/min up to 1600°C under dry air atmosphere. The dimensional change was measured *in situ* using pure alumina probes with a load less than 0·02 N, which corresponds to a pressure of less than 0·25 kPa. The final density was measured by the Archimedes method. The relative density ρ and its temperature derivative $d\rho/dT$ were calculated from the final density and the continuously measured shrinkage; they are plotted as functions of temperature T. Apparent activation energies at several densities were calculated from Arrhenius plots of the densification rates at different heating rates.[16]

The morphology of the powders was observed by transmission electron microscopy (TEM). The microstructure of powder compacts at various stages of heat treatments was observed by scanning electron microscopy (SEM). Specimens with grain sizes larger than 1 μm were observed on polished and thermally etched surfaces, while those with grain sizes less than 1 μm were observed on fractured surfaces to avoid grain growth during thermal etching.

3 Results

3.1 Powder agglomeration and green bodies

Figure 2 shows the powder morphology observed by TEM. Both BO and TA powders consisted mainly of submicron-sized primary particles with diameters of 0·1 μm or less. Agglomerates of these particles had larger sizes and more irregular shapes for the BO powders than for the TA powders and this indicates that the size distribu-

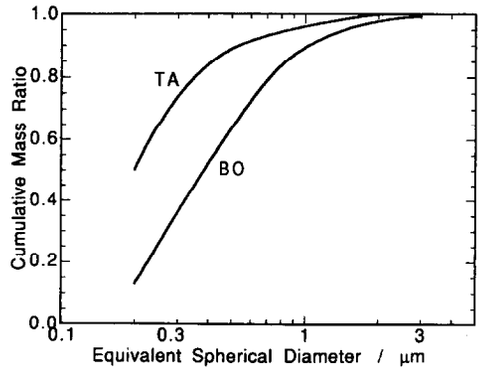

Fig. 1. Particle size distributions of BO and TA powders given by the suppliers.

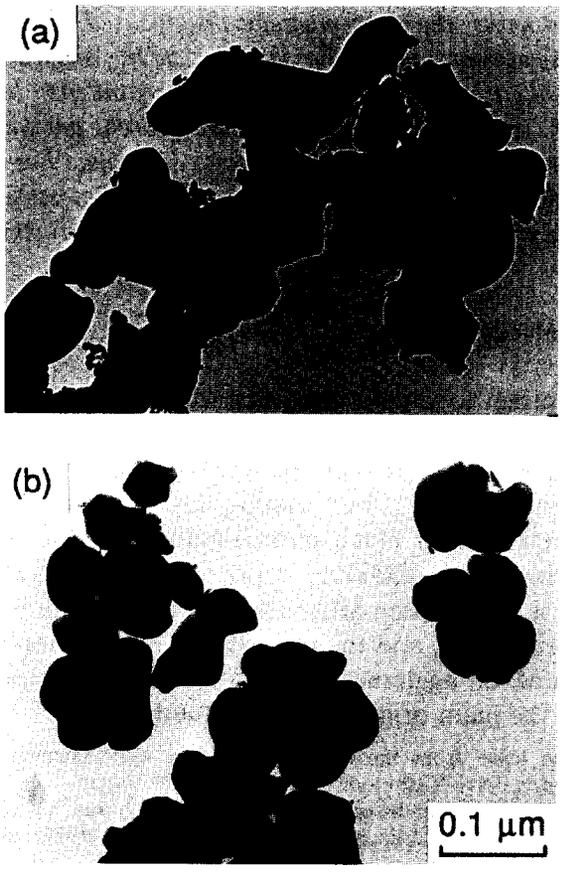

Fig. 2. Transmission electron micrographs of (a) BO and (b) TA powders.

tion shown in Fig. 1 was of agglomerates.

In addition to these primary particles, the BO powders have another kind of very fine particle with diameters of about 10 nm (they are referred to as nano-sized particles). A few nano-sized particles are also observed in the micrograph of the TA powders. These particles contained no metallic element other than aluminum based on the energy dispersion analysis of X-ray in TEM, although they were too small to determine their crystal structure. As the size is similar to the typical of γ-alumina, they might be non-transformed γ-alumina.

After CIP, the BO and TA powder compacts had relative densities of 0·481 and 0·566, respectively. This difference in green density is attributed to the difference in agglomerate size and morphology; in the BO powder compacts, the irregular shape of agglomerates made the packing more difficult.

3.2 Initial stage of sintering

General densification behavior at a constant heating rate is illustrated in Fig. 3: (a) is for the BO powders and (b) is for the TA powders. At low temperatures around 1100°C, a shoulder was observed on the densification rate curve of an as-CIPed BO powder compact (Fig. 3 (a)). The

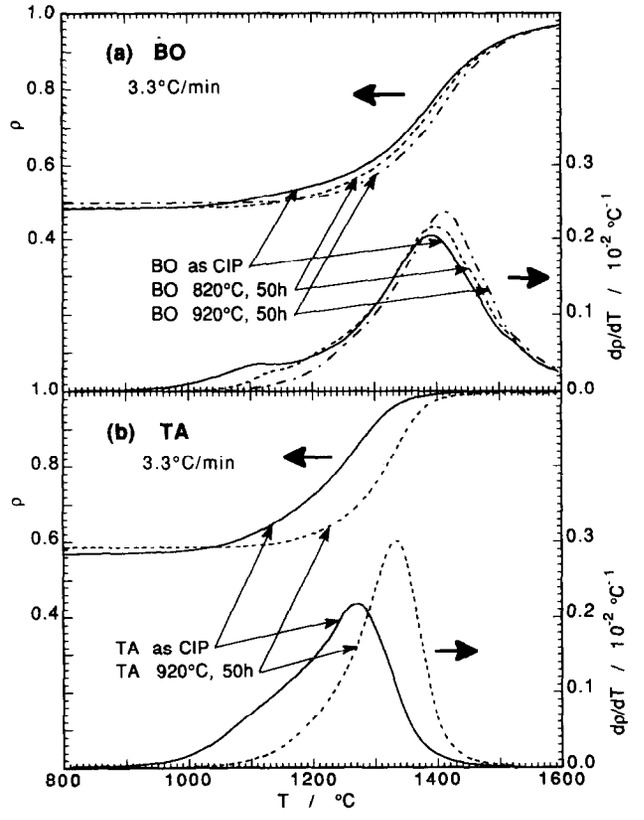

Fig. 3. Densification curves during sintering at a heating rate of 3·3°C/min for powder compacts of (a) BO and (b) RA with and without pre-treatment. The upper and lower curves in both (a) and (b) are the relative densities, ρ, and their temperature derivatives, $d\rho/dT$, respectively.

observation of such a shoulder has already been reported by the authors.[17] The shoulder became very small after the pre-treatment at 820°C for 50 h and disappeared almost completely after 50 h at 920°C. This shoulder was shifted towards lower temperatures with decreasing heating rate (not shown in Fig. 3(a)), implying a thermally activated process. For an as-CIPed TA powder compact, a much less distinct shoulder on the main peak was observed at almost the same temperature as the shoulder for the BO powder compact (Fig. 3 (b)). This shoulder also disappeared after the pre-treatment at 920°C for 50 h.

Figure 4 shows the microstructural developments during the pre-treatment and/or the initial stage sintering corresponding to the shoulder of BO powder compacts observed by SEM. The nano-sized particles observed by SEM are seen as small bright spots in the as-CIPed compact along with many large particle agglomerates of 0·1 to 0·3 μm (Fig. 4(a)). A particle network of the large agglomerates of about 0·3 μm is seen in this micrograph. After sintering up to the end of the shoulder, more than half of the nano-sized particles disappeared (Fig. 4 (b)). After the pre-treatment at 920°C for 50 h, almost all of the nano-sized particles disappeared (Fig. 4 (c)). In addition, the agglomerates of the primary particles show rather rounded morphology and seem to have a narrower size distribution. During all of these treatments the large agglomerates making up the particle network remain at a very similar size of about 0·3 μm.

Figure 5 shows the microstructural developments during the pre-treatment of the TA powder compacts. Compared to the as-CIPed TA compacts (Fig. 5(a)) the pre-treated TA compact consisted of more uniform but much larger particles (Fig. 5(b)).

In both the BO and TA powder compacts, the nano-sized particles disappear during low temperature annealing, i.e. during the shoulder in the initial stage sintering or during the pre-treatment. Their disappearance appears to be as a result of mass transport from them onto or into the submicron-sized particles which they contact. Among diffusional mechanisms considered normally, volume and grain boundary diffusions contribute to both densification and coarsening, while surface diffusion contributes only to coarsening and has the lowest values of activation energy and power index of particle size.[3] It means a process controlled by surface diffusion is more likely at lower temperatures and for finer particles. The dominant mechanism for the disappearance of the nano-sized particles could not, however, be determined clearly because the apparent activation energy

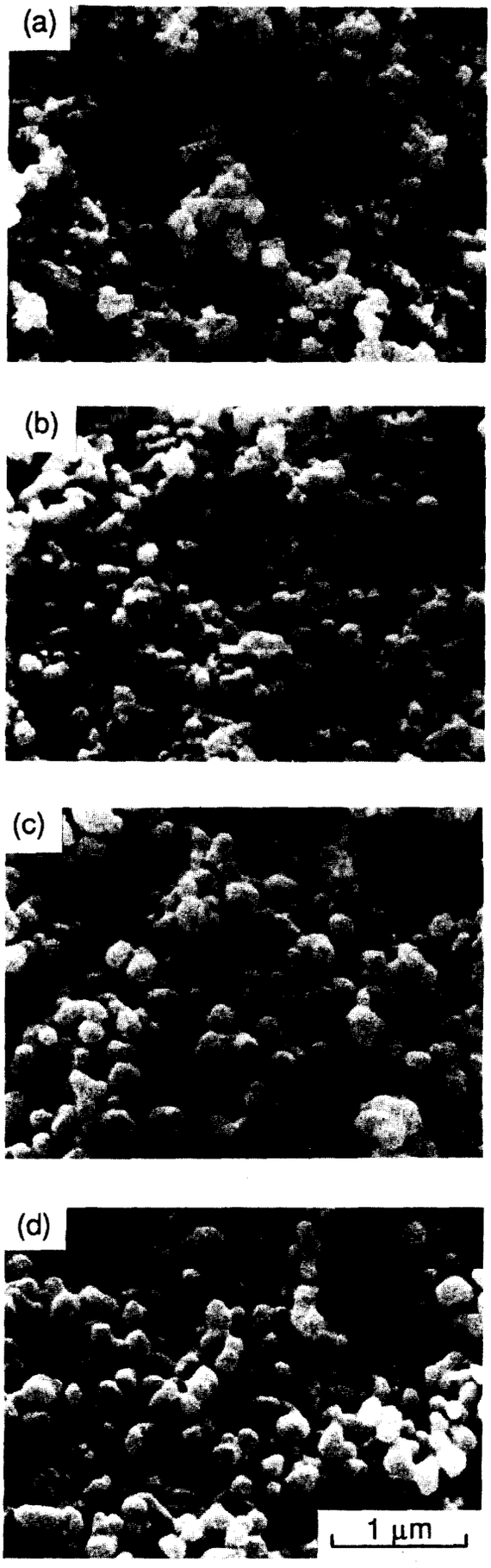

Fig. 4. Scanning electron micrographs of fracture surfaces of BO powder compacts: (a) as compacted, (b) sintered at 3·3°C/min until 1160°C, (c) pre-treated at 920°C for 50 h, and (d) sintered at 3·3°C/min until 1160°C with pre-treatment at 920°C for 50 h.

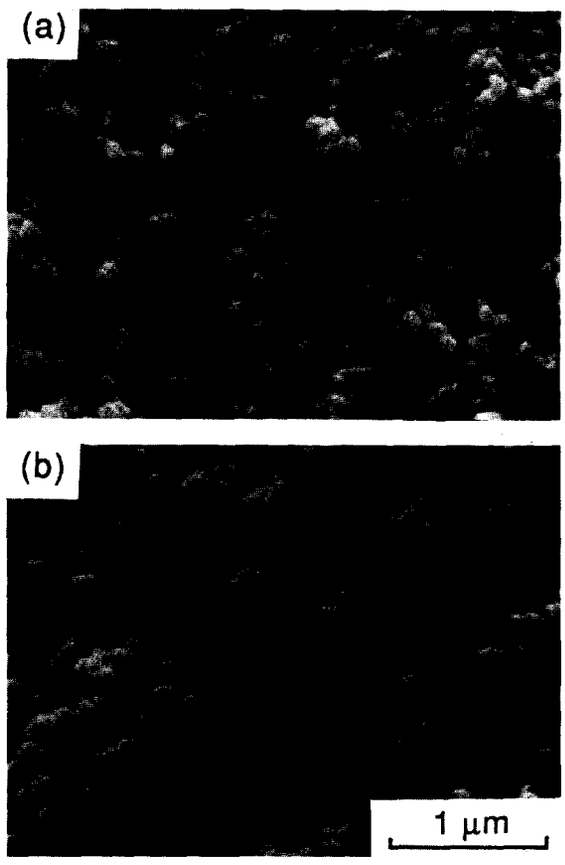

Fig. 5. Scanning electron micrographs of fracture surfaces of TA powder compacts: (a) as compacted, (b) pre-treated at 920°C for 50 h.

could not be measured, as described in the following paragraph.

Using the logarithmic plot of $T(\mathrm{d}(\Delta L/L_0)/\mathrm{d}T)$, which equals $-(T/3\rho_0)(\mathrm{d}\rho/\mathrm{d}T)$, versus $1/T$, Young & Cutler[15] obtained the apparent activation energy for the initial stage of sintering. Here $\Delta L/L_0$ is the relative change in length of the compact. Because their powder was coarser than 1 μm, there was negligible grain growth during this stage. Unfortunately, the significant grain growth of the present powder compacts does not allow a calculation of the apparent activation energy by their method.

3.3 Intermediate stage of sintering

The pre-treatment at 920°C for 50 h shifted the main densification rate peak toward higher temperatures by 60°C and raised its height by 36% in TA powder compacts (Fig. 3(b)), while it shifted the peak by only 20°C and raised the height by only 15% in BO powder compacts (Fig. 3(a)). Because the pre-treatment did not significantly coarsen the large agglomerates which made up the particle network for the as-CIPed BO powder compacts, as already mentioned, it did not cause a big change in the sintering behavior of the BO powder compacts. On the other hand, the pre-

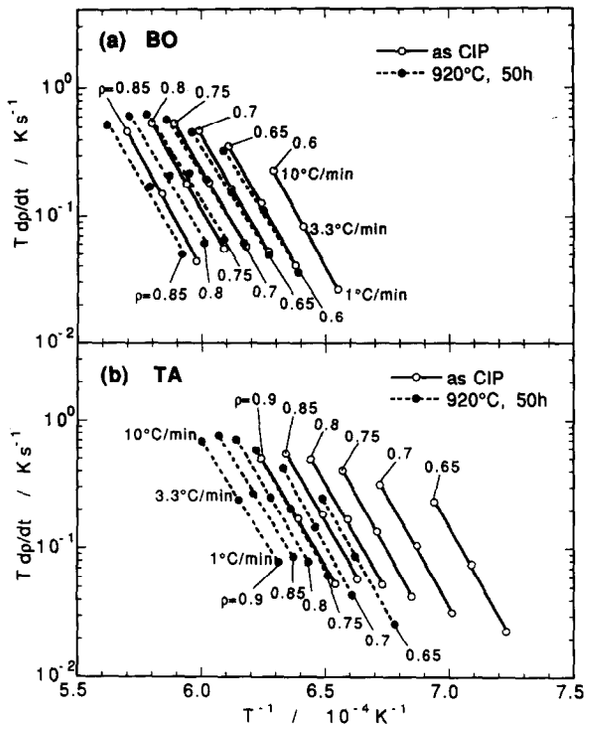

Fig. 6. Arrhenius plots of constant heating rate sintering of powder compacts (a) BO and (b) TA, with and without pre-treatment.

treatment strongly shifted the main densification peak to higher temperatures in TA powder compacts because the agglomerates coarsened very much during the treatment. The average grain size in TA powder compacts was still smaller than in BO, resulting in the lower temperature of the main densification peak.

The peaks were shifted toward lower temperatures with decreasing heating rates, as expected for a thermally activated process (not shown in Fig. 3). Figure 6 shows the Arrhenius plots of densification rates at different heating rates. In the intermediate stage of sintering, the apparent activation energies were 653 and 617 kJ/mol for the as-CIPed and pre-treated BO powder compacts, respectively, and 650, and 638 kJ/mol for those of the TA powder compacts. These values were obtained in the region of relative density from 0·65 to 0·80 for BO samples and from 0·70 to 0·85 for TA samples, where the effect of the shoulder was no longer apparent. In these regions grains did grow, but the sizes at a given density were almost identical among the compacts heated at different rates, which is indispensable for estimating the apparent activation energy. The little effect of pre-treatment on the apparent activation energy for both BO and TA powder compacts implies no change in the rate-controlling mechanism in the intermediate stage of sintering.

3.4 Final microstructure

Figure 7 shows the final microstructure of the BO materials with and without pre-treatments. The three samples shown in Fig. 7 had the same final density of 0·970 after sintering up to 1600°C at 3·3°C/min. These three had the same mean grain size of 1·9 μm; it was calculated as 1·38 times the mean intercept area on a plane section of more than 1000 grains observed in five different positions for each sample. Compared at the same sintering condition and the same density, the pre-treatment had no significant influence on the final microstructure in BO ceramics.

As already seen in Fig. 3 (b), the TA powder

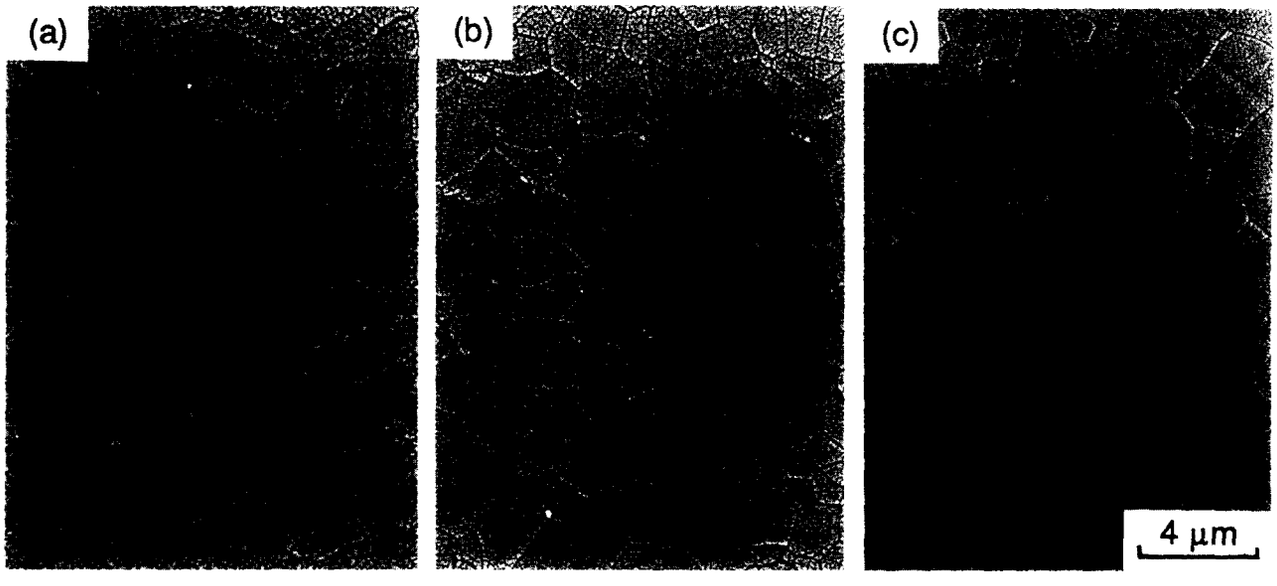

Fig. 7. Scanning electron micrographs of polished and thermally etched surfaces of BO ceramics sintered with 3·3°C/min until 1600°C: (a) without pre-treatment, (b) with pre-treatment at 820°C for 50 h, and (c) with pre-treatment at 920°C for 50 h. All of these specimens have the same final density of 0·97.

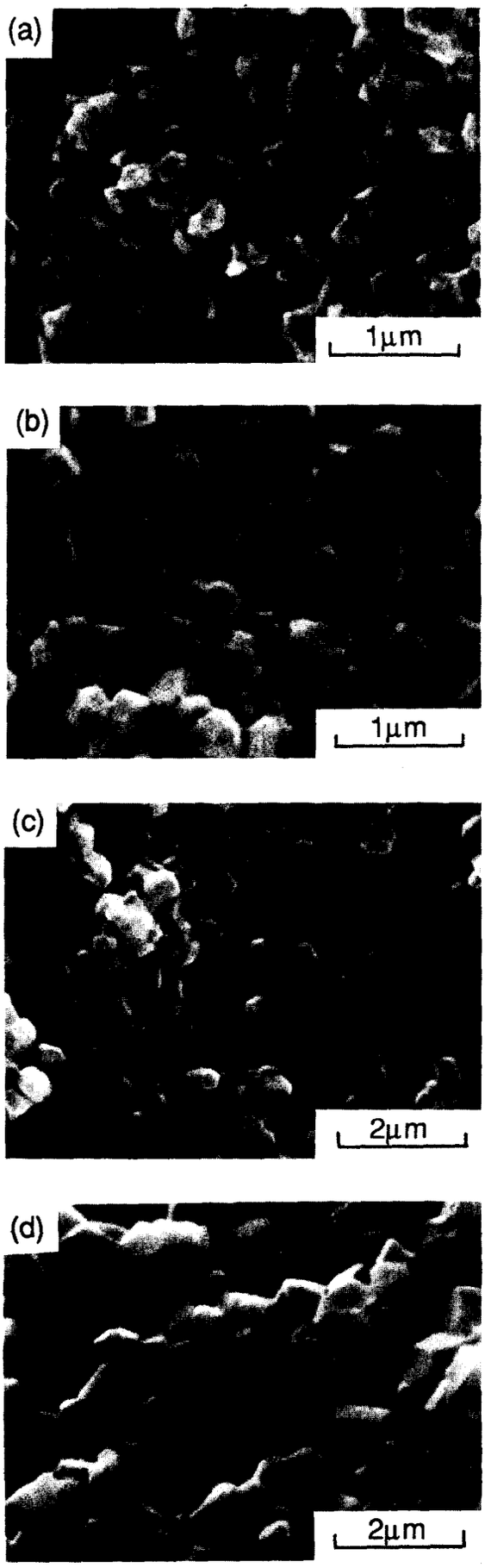

Fig. 8. Scanning electron micrographs of fracture surfaces of TA ceramics sintered at 3·3°C/min: (a) sintered up to 1290°C, (b) sintered up to 1350°C with a pre-treatment at 920°C for 50h, (c) sintered up to 1375°C, and (d) sintered up to 1430°C with the pre-treatment. Both (a) and (b) have the same final density of 0·89, and both (c) and (d) have that of 0·99.

compacts without and with pre-coarsening treatment reached the final density of 0·998 and 0·995, respectively, at about 1500°C: no more densification occurred in the sintering above this temperature. For this powder, pre-treatment decreased the highest density which a compact can achieve. The microstructures at certain densities lower than 0·995 are shown in Fig. 8, by interrupting the sintering cycle: (a) and (b) are microstructures at the density of 0·890, without and with pre-treatment, respectively, and (c) and (d) are at the density of 0·990. Here, fracture surfaces were observed because microstructures finer than 1 μm grain size easily coarsen during thermal etching. When comparing samples of the same density but different sintering temperature, the pre-treatment made the final microstructure coarser in the TA powder compacts.

4 Discussion

After pre-treatments, the nano-particles disappeared, resulting in disappearance of the initial shoulder in the densification rate curves in the subsequent sintering. For the BO powder compacts, however, the size of the large agglomerates which made up the particle network remained very similar during the pre-treatment, leading to little influence on the sintering behavior in the intermediate stage and the final microstructure. For the TA powder compacts, a coarsening of the agglomerates of the primary particles took place during the pre-treatments. The size increase influenced the sintering behavior in the intermediate stage and the final microstructure. Here we discuss these effects based on the results of TA powder compacts.

Firstly, the particle size increase in the treatment resulted in the shift of the main densification peak toward higher temperature as already mentioned. In addition to the temperature shift, the height of the main densification peak was raised by the treatment. Although the height of the densification peak has not been discussed in detail in the literature to the knowledge of the authors, it can be deduced that the narrower the size distribution, the higher the peak should be, providing all other conditions are identical. The height change in the TA powder compact data is qualitatively explained by a narrowing of the particle size distribution.

The effect of the pre-treatment, an increase in the height of the main densification rate peak, is the opposite to the policy of 'rate-controlled sintering,[14] which tries to avoid rapid shrinkage by decreasing the heating rate in the intermediate stage. Rapid shrinkage is expected to introduce

large closed pores inside the sintered body by differential densification. This explains why for TA powder compacts the sintered body with the pre-treatment could reach the final density a little lower than that achieved without the pre-treatment, and had a coarser microstructure when compared at the same density. In contrast, powders with narrow size distributions produced by colloidal techniques are not agglomerated to some extent and more regularly packed, resulting in a higher final density than powders with larger size distributions.[9,11,12]

In contrast to a coarsening effect of the pre-treatments for the final microstructure as seen for the TA powders, Chu *et al.* reported finer microstructures for conventional grade alumina and magnesia powders and high-grade alumina powders.[13] The conventional grade powder compacts revealed abnormal grain growth at the final stage (see Figs 6 and 7* of Ref. 13; Figs 7(c) and (d) must be placed in reverse order). Abnormal grain growth starts at a certain stage of annealing when some of the largest grains start to grow quickly by absorbing the surrounding grains. The more uniform the microstructure, the more strongly the onset of abnormal grain growth is retarded: this could be the microstructural fining effect found by Chu *et al.*

In the case of the high-grade powder compacts, Chu *et al.* reported that the sintered body with pre-treatment gave a finer final microstructure than without under the same sintering conditions.[13] Because the pre-treatment delays densification, an as-CIPed compact arrives at the final stage of sintering sooner (where coarsening is predominant[3]) than a pre-treated compact. For example, the TA powder compacts with and without pre-treatment showed grain sizes of 5 and 8 μm, respectively, after the sintering with 3·3°C/min up to 1600°C. This could also explain the microstructural fining effect found by Chu *et al.*

5 Conclusions

The commercial, non-doped α-alumina powders used in this study contained some nano-sized alumina particles (10 nm) as well as submicron-sized primary particles (0·1 μm), which agglomerated into diameters of 0·2–0·4 μm. The powder with many of these nano-sized particles showed a low temperature shoulder in densification rate curves of constant heating rate sintering while for the powder with fewer nano-sized particles the shoulder was less marked. The nano-sized particles disappear almost completely after a pre-treatment, resulting in the disappearance of the shoulder in the subsequent densification rate curves.

When the size of the large agglomerates which made up the particle network remained similar during the pre-treatment, the treatment had little influence on the intermediate and final stage sintering (BO powder). On the other hand when the growth of the agglomerates of the primary particles took place during the pre-treatments, the treatments shifted the main densification rate peak toward higher temperatures and raised its height (TA powder). The treatments, however, caused little change in the apparent activation energy, implying no change in the rate-controlling mechanism in the intermediate stage sintering. Because the treatments caused more rapid shrinkage in the intermediate stage, the sintered body with the treatment had coarser microstructure than the body with it when compared at the same density.

Finally, it was pointed out that pre-treatments have the possibility to retard the onset of abnormal grain growth by creating a more uniform microstructure before densification begins.

Acknowledgment

Helpful comments and discussion about powder agglomeration from Dr Paul Bowen, Laboratoire de Technologie des Poudres, EPFL, are gratefully acknowledged.

References

1. Harmer, M. P., Science of sintering as related to ceramic powder processing. In *Ceramic Transactions Vol. 1, Ceramic Powder Science II*, ed. G. L. Messing *et al.* American Ceramic Society, 1991, pp. 824–39.
2. Aeraback, R. S., Höfler, H. J., Hahn, H. & Logar, J. C., Sintering and grain growth in nanocrystalline ceramics. *Nanostructured Mater.*, **1** (1992) 173–8.
3. Shaw, N. J., Densification and coarsening during solid state sintering of ceramics: a review of models. *Powder Metallurgy Int.*, **21** (1989) 16–21.
4. Gray, W. A., *The Packing of Solid Particles*. Chapman and Hall, London, 1968.
5. Messing, G. L. & Onoda, Jr, G. Y., Sintering of inhomogeneous binary powder mixtures. *J. Am. Ceram. Soc.*, **64** (1981) 468–72.
6. Smith, P. & Messing, G. L., Sintering of bimodally distributed alumina powders. *J. Am. Ceram. Soc.*, **67** (1984) 238–42.
7. Yeh, T.-S. & Sacks, M. D., Effect of particle size distribution on the sintering of alumina. *J. Am. Ceram. Soc.*, **71** (1988) C484–7.
8. O'Hara, M. J. & Cutler, I. B., Sintering kinetics of binary mixtures of alumina powders. *Proc. Brit. Ceram. Soc.*, **12** (1969) 145–54.
9. Lange, F. F., Powder processing science and technology for increased reliability. *J. Am. Ceram. Soc.*, **72** (1989) 3–15.
10. Yan, M. F., Cannon, Jr, R. M., Bowen, H. K. & Chowdhry, U., Effect of grain size distribution on sintered

density. *Mater. Sci. Eng.*, **60** (1983) 275–81.
11. Barringer, E. A. & Bowen, H. K., Formation, packing, and sintering of monodisperse TiO_2 powders. *J. Am. Ceram. Soc.*, **65** (1982) C199–201.
12. Hay, R. A., Moffatt, W. C., & Bowen, H. K., Sintering behaviour of uniform-sized α-Al_2O_3 powder. *Mater. Sci. Eng.*, **A108** (1989) 213–19.
13. Chu, M-Y., De Jonghe, L. C., Lin, M. K. F. & Kin, F. J. T., Precoarsening to improve microstructure and sintering of powder compacts. *J. Am. Ceram. Soc.*, **74** (1991) 2902–11.
14. Palmour III, H., Rate controlled sintering for ceramics and selected powder metals. In *Science of Sintering*, ed. D. P. Uskovic *et al.* Plenum Press, 1989, pp. 337–56.
15. Young, W. S. & Cutler, I. B., Initial sintering with constant rates of heating. *J. Am. Ceram. Soc.*, **53** (1970) 659–63.
16. Wange, J. & Raj, R., Estimation of the activation energies for boundary diffusion from rate-controlled sintering of pure alumina, and alumina doped with zirconia or titania. *J. Am. Ceram. Soc.*, **73** (1990) 1172–5.
17. Sato, E. & Carry, C., Effect of yttrium doping on sintering behaviour of fine grained alumina. In *Third Euro-Ceramics*, Vol 1, ed. P. Duran & J. F. Fernandez. Faenza Editrice Ibérica, 1993, pp. 691–6.